Journal of Statistical Physics, Vol. 66, Nos. 1/2, 1992

Partition Function Zeros for the One-Dimensional Ordered Plasma in Dirichlet Boundary Conditions

J. Roumeliotis[1,2] **and E. R. Smith**[1,3]

Received March 26, 1991

We consider the grand canonical partition function for the ordered one-dimensional, two-component plasma at fugacity ζ in an applied electric field E with Dirichlet boundary conditions. The system has a phase transition from a low-coupling phase with equally spaced particles to a high-coupling phase with particles clustered into dipolar pairs. An exact expression for the partition function is developed. In zero applied field the zeros in the ζ plane occupy the imaginary axis from $-i\infty$ to $-i\zeta_c$ and $i\zeta_c$ to $i\infty$ for some ζ_c. They also occupy the diamond shape of four straight lines from $\pm i\zeta_c$ to ζ_c and from $\pm i\zeta_c$ to $-\zeta_c$. The fugacity ζ acts like a temperature or coupling variable. The symmetry-breaking field is the applied electric field E. A finite-size scaling representation for the partition in scaled coupling and scaled electric field is developed. It has standard mean field form. When the scaled coupling is real, the zeros in the scaled field lie on the imaginary axis and pinch the real scaled field axis as the scaled coupling increases. The scaled partition function considered as a function of two complex variables, scaled coupling and scaled field, has zeros on a two-dimensional surface in a domain of four real variables. A numerical discussion of some of the properties of this surface is presented.

KEY WORDS: Partition function zeros; mean field transition; one-dimensional plasma.

1. INTRODUCTION

The grand canonical partition function for a finite-size system may be considered as a function of complex temperature and complex fugacity. For a system with a liquid–gas transition the temperature acts as a scaled coupling variable and the chemical potential (or logarithm of the fugacity)

[1] Mathematics Department, La Trobe University, Bundoora, Victoria 3083, Australia.
[2] Mathematics Department, University College, Australian Defence Forces Academy, Campbell, ACT, 2601, Australia.
[3] Mathematics Department, Odense University, 5230 Odense M, Denmark.

0022-4715/92/0100-0233$06.50/0

acts as a symmetry-breaking external field. For hard-core systems, the partition function is a polynomial in the fugacity and so has a finite number of zeros in the complex fugacity plane, as pointed out by Yang and Lee.[1] As the system becomes large, these zeros may coalesce onto arcs in the fugacity plane. If these arcs intersect the real positive axis in the thermodynamic limit, the system has a phase transition. For the ferromagnetic Ising model (or attractive potential lattice gas) Lee and Yang[2] showed that the zeros exhibit precisely this behavior with the arc being a segment of the unit circle. Later work by Penrose[3] showed that similar behavior may be expected for any system with a sufficiently repulsive core in the interparticle interaction. Fisher later introduced the idea of studying the zeros of the grand canonical partition function in the complex temperature and displayed these zeros explicitly for a two-dimensional ferromagnetic Ising model in zero field.[4] The partition function may be considered as a function of two complex variables, fugacity and temperature. The zeros in fugacity and temperature, for finite systems, determine the singularity structure of the pressure (or free energy). Thus far there has been little discussion of the zero surface in the two complex variables.

For Coulombic systems the situation is a little more complicated. Forrester[5,6] has evaluated the partition function for a two-component, one-dimensional plasma with a logarithmic potential and showed that this system has a plasma phase to dipolar phase transition. For coupling appropriate to the plasma phase the fugacity zeros lie on arcs which allow the zeros to cluster near the origin. In the thermodynamic limit the zero density is finite in any neighborhood of the origin. For coupling appropriate to the dipolar phase, the zeros withdraw from the origin, but an arc of zeros cuts the positive real fugacity axis. Thus, while for many systems the physically interesting part of the zero distribution is around the critical fugacity on the real positive axis, for Coulombic systems the whole zero distribution is of interest.

For a system with a phase transition at temperatures and fugacities close to their critical values, one can construct a finite-size scaling theory representation of the partition function with the deviations of temperature and fugacity from their critical values scaled with the fractional powers of the system volume. Recently Itzykson *et al.*[7] and Glasser *et al.*[8] have developed a theory which connects the distribution of zeros of this scaled partition function as a function of scaled coupling to the critical behavior of the thermodynamic free energy density at critical fugacity. Glasser *et al.*[9] illustrate this theory by considering the finite-size scaling partition function for a system with a generic mean field transition at critical fugacity. They were able to write this partition function in terms of a $K_{1/4}$ Bessel function and thus identify its zeros in the complex scaled coupling plane.

In this paper we consider a one-dimensional neutral system of point charged particles which maintain the order $-+-+\cdots-+$ on the line. The potential energy is derived from solutions of the one-dimensional Poisson equation. This system has been discussed by Smith and Forrester[10] in free and in periodic boundary conditions. In free boundary conditions the system has no phase transition and the grand canonical partition function, considered as a function of fugacity ζ, has zeros on $(-i\infty, -i\zeta_c]$ and $[i\zeta_c, i\infty)$ for a particular real ζ_c. The fugacity in this system is part of a dimensionless coupling parameter and the system is never in a plasma like state. In periodic boundary conditions the system does have a phase transition from a low-coupling phase in which the particles are equally spaced on average to a high-coupling phase in which the particles bind into dipolar pairs. Smith and Forrester showed that the finite-size scaled partition function as a function of complex scaled coupling had the same zero structure as found by Glasser *et al.*[9]

The natural symmetry-breaking field for this transition is an applied electric field. It is not entirely clear how such a field can be applied in periodic boundary conditions. Thus in the next section we describe the Hamiltonian for the system in Dirichlet boundary conditions, for which it is simple to include an applied electric field. In zero field the Hamiltonian is the same as in periodic boundary conditions. With or without external field, the calculation of the grand canonical partition function proceeds exactly as in periodic boundary conditions and the results are reported. In Section 3 the zeros of the zero-field partition function in the whole complex coupling plane are described. In the complex ζ (fugacity) plane these zeros lie on the imaginary axis on $(-i\infty, -i\zeta_c]$ and $[i\zeta_c, i\infty)$ and also on the square with corners at $\pm i\zeta_c$ and $\pm\zeta_c$. Here ζ_c is a real critical fugacity value. In Section 4 the finite-size scaled partition function as a function of scaled coupling and scaled external electric field is derived. This scaled partition function is of mean field type. In zero scaled external field it is exactly the generic mean field partition function studied by Glasser *et al.*[9] We develop asymptotic expansions for the zeros in complex scaled applied electric field with zero scaled coupling. Numerical studies then show that as the coupling increases, the zeros pinch the real axis. The field zeros are always pure imaginary for real coupling. In Section 5 the motion of the field zeros as the scaled coupling varies in the complex plane is described. The results are mainly numerical, but the motions are very complicated, even in this mean field case.

2. THE SYSTEM

We consider a system of $2N$ charged particles with particle j having charge $q_j = Qe_j$, $e_j = (-1)^j$, $1 \leqslant j \leqslant 2N$. The particles are in an ensemble which maintains their ordering on the line $-L/2 \leqslant x \leqslant L/2$. Thus, the coordinates of the particles $x_1, ..., x_{2N}$ obey the constraints

$$-L/2 \leqslant x_1 \leqslant x_2 \in x_3 \cdots \leqslant x_{2N-1} \leqslant x_{2N} \leqslant L/2 \tag{2.1}$$

The electrostatic potential $\Psi(x)$ in the system is the solution of the one-dimensional Dirichlet problem

$$\Psi''(x) = -2Q \sum_{j=1}^{2N} e_j \, \delta(x - x_j) \tag{2.2}$$

on $L/2 < x < L/2$ with the boundary conditions

$$\Psi(\pm L/2) = \mp E_0 L/2 \tag{2.3}$$

where E_0 is the applied electric field. It is convenient to define

$$M = \sum_{j=1}^{2N} e_j x_j \tag{2.4}$$

so that the dipole moment of a configuration $\{x_1, x_2, ..., x_{2N}\}$ is QM. The solution to the Dirichlet problem is

$$\Psi(x) = -Q \sum_{k=1}^{2N} e_k |x - x_k| - (2QM/L + E_0)x \tag{2.5}$$

The Hamiltonian for the system may then be written

$$\mathscr{H}_{\mathrm{DIR}}(E_0) = -\frac{1}{2} Q^2 \sum_{j=1}^{2N} \sum_{k=1}^{2N} e_j e_k |x_j - x_k| - Q^2 M^2/L - E_0 QM \tag{2.6}$$

With $\beta = 1/kT$, and the scaled variables

$$\gamma = Q^2/kT, \qquad \omega = E_0 Q/kT \tag{2.7}$$

this Hamiltonian may be simplified, using the ordering condition (2.1), to

$$\beta \mathscr{H}_{\mathrm{DIR}}(E_0) = -\gamma M^2/L + (\gamma - \omega) M \tag{2.8}$$

In zero field ($\omega = 0$) this is exactly the Hamiltonian for the system in periodic boundary conditions: the partition function evaluation techniques of Smith and Forrester[10] may be applied. We write

$$\mathbb{Z}_{2N}(L, \gamma, \omega) = \exp[-\gamma L(1 - \omega/\gamma)^2/4] \, \mathbb{F}_{2N}(L, \gamma, \omega) \tag{2.9}$$

for the canonical partition function, where

$$\mathbb{F}_{2N}(L, \gamma, \omega) = \int_0^L dx_{2N} \int_0^{x_{2N}} dx_{2N-1} \cdots \int_0^{x_2} dx_1 \exp\left\{\frac{\gamma}{L}\left[M - \frac{L}{2}\left(1 - \frac{\omega}{\gamma}\right)\right]^2\right\} \tag{2.10}$$

We first introduce

$$\mathbb{G}_{2N}(L, \alpha) = \int_0^L dx_{2N} \int_0^{x_{2N}} dx_{2N-1} \cdots \int_0^{x_2} dx_1 \exp(-\alpha M) \tag{2.11}$$

which has a Laplace transform with respect to L given by

$$\hat{G}_{2N}(s, \alpha) = \frac{1}{s}\left[s(s+\alpha)\right]^{-N} \tag{2.12}$$

We then use the identity

$$\exp(\lambda x^2) = (\pi\lambda)^{1/2} \int_{-\infty}^{\infty} du \exp(-u^2/\lambda + 2ux) \tag{2.13}$$

with $\lambda = \gamma/L$ and $x = [M - \frac{1}{2}(1 - \omega\gamma)]$, to write $\hat{\mathbb{F}}_{2N}$ in terms of an integral over u on $(-\infty, \infty)$ of $\hat{G}_{2N}(s, -2u)$. The grand canonical partition function is then

$$\Xi(\zeta, L, \gamma, \omega) = \sum_{N=0}^{\infty} \zeta^{2N} \mathbb{F}_{2N}(L, \gamma, \omega) \tag{2.14}$$

If we insert the representation of $\mathbb{Z}_{2N}(L, \gamma, \omega)$ in terms of the inverse transform of $\hat{F}_{2N}(\zeta, \gamma, \omega)$, add up the sum, calculate the inverse transform in terms of the residues at $s_\pm = u \pm (u^2 + \zeta^2)^{1/2}$, and manipulate the result a little, we obtain

$$\begin{aligned}\Xi(\zeta, L, \gamma, \omega) &= \frac{1}{2}\left(\frac{L}{\gamma\pi}\right)^{1/2} \exp\left(-\frac{\gamma L(1-\omega/\gamma)^2}{4}\right) \int_{\infty}^{\infty} du \left(1 + \frac{\omega}{\gamma} - \frac{2u}{\gamma}\right) \\ &\quad \times \exp\left(-\frac{Lu^2}{\gamma} + \frac{l\omega u}{\gamma}\right) \{\exp[L(u^2+\zeta^2)^{1/2}] + \exp[-L(u^2+\zeta^2)^{1/2}]\}\end{aligned} \tag{2.15}$$

This partition function displays a phase transition of mean field type in zero field. Details may be found in Smith and Forrester.[10] The low-coupling

phase has $p/\rho kT = 1/2$ for $\Gamma = Q^2/2\rho kT \geqslant 1$ and $p/\rho kT = 1 - \Gamma/2$ for $0 \leqslant \Gamma \leqslant 1$. The low coupling phase ($0 \leqslant \Gamma \leqslant 1$) has the particles spread out uniformly with average spacing $L/2N$. In the high-coupling phase the particles coalesce into small dipole moment pairs ($-+\ \ -+\ \ -+\cdots-+$) or large dipole moment pairs ($-\ \ +-\ \ +-\cdots+-\ \ +$) with low and high dipole moment density, respectively. The symmetry-breaking field for this transition is the external applied electric field E_0.

3. ZEROS AT ZERO FIELD

In this section we consider the zeros of Ξ in he complex $\xi = \zeta/\gamma$ plane in zero field. We change the variable of integration in (2.15) to $v = u/\gamma$ and put $\omega = 0$, $l = \gamma L$, and $\xi = \zeta/\gamma$. We obtain

$$\Xi(\gamma\xi, l/\gamma, \gamma, 0) = \tfrac{1}{2}(L\gamma/\pi)^{1/2} \exp(-l/4)\, \chi(\xi, l) \tag{3.1}$$

with

$$\chi(\xi, l) = \int_{-\infty}^{\infty} e^{lg_1(v)} + e^{lg_2(v)}\, dv \tag{3.2}$$

and

$$g_1(v) = (v^2 + \xi^2)^{1/2} - v^2; \qquad g_2(v) = -(v^2 + \xi^2)^{1/2} - v^2 \tag{3.3}$$

The zeros of Ξ are then the zeros of $\chi(\xi, l)$ and we study these zeros as $l \to \infty$, so that we may estimate χ by the method of steepest descents.

The steepest descent evaluation gives contributions to χ for some or all of the saddle points of g_1 and g_2. These saddle points are at

$$\text{for } g_1\text{:}\quad g_1'(v_j) = 0,\ j = -1, 0, 1 \text{ with } v_{\pm 1} = \pm(\tfrac{1}{4} - \xi^2)^{1/2},\ v_0 = 0 \tag{3.4a}$$

$$\text{for } g_2\text{:}\quad g_2'(v) = 0 \text{ only for } v = 0 \tag{3.4b}$$

The square root is defined so that $g_2'(v) = 0$ has only the solution $v = 0$. Notice that $\chi(\xi, l)$ is even in ξ, so that if ξ_0 is a zero, $-\xi_0$ is a zero. Further notice that with the asterisk representing complex conjugation, $\chi^*(\xi, l) = \chi(\xi^*, l)$. Thus, if ξ_0 is a zero, ξ_0^* is also a zero. This means that we may find all the zeros of $\chi(\xi, l)$ by considering $\mathrm{Re}(\xi) \geqslant 0$, $\mathrm{Im}(\xi) \geqslant 0$. For $\xi = \sigma + i\tau$ with $\sigma \geqslant 0$, $\tau \geqslant 0$, we cut the complex v plane from $-\tau + i\sigma$ to $-\tau + i\infty$ and from $\tau - i\sigma$ to $\tau - i\infty$. At the saddle points we have

$$g_1(v_0) = \xi, \qquad g_2(0) = -\xi, \qquad g_1(v_{\pm 1}) = \tfrac{1}{4} + \xi^2 \tag{3.5}$$

and the second derivatives

$$g_1''(v_0)=\frac{1}{\xi}-2, \qquad g_2''(0)=-\frac{1}{\xi}-2, \qquad g_1''(v_{\pm 1})=8\left(\xi^2-\frac{1}{4}\right). \quad (3.6)$$

A zero of χ may arise in one of two ways:

(i) The saddle point v_0 of g_1 dominates those at $v_{\pm 1}$, and the contribution of the integral over $\exp[lg_1(v)]$ cancels the contribution of the integral over $\exp[lg_2(v)]$. This requires

$$\mathrm{Re}[g_1(v_0)] > \mathrm{Re}[g_1(v_{\pm 1}] \quad (3.7a)$$

and

$$\mathrm{Re}[g_1(v_0)] = \mathrm{Re}[g_2(0)] \quad (3.7b)$$

Setting $\xi=\sigma+i\tau$ again, Eq. (3.7a) gives

$$|\tau| > |\sigma-\tfrac{1}{2}| \quad (3.7c)$$

while Eq. (3.7b) gives $\sigma=-\sigma$, so that this type of zero can only occur when $\sigma=0$ and $|\tau|>1/2$.

(ii) The saddle points v_0 and $v_{\pm 1}$ must all be on the contour of steepest descent and we must have

$$\mathrm{Re}[g_1(v_{\pm 1})] = \mathrm{Re}[g_1(v_0)] \Rightarrow (\sigma-\tfrac{1}{2})^2-\tau^2=0 \quad (3.8a)$$

and these saddle points must dominate that of g_2 at $v=0$. This requires

$$-\sigma < \sigma \quad (3.8b)$$

which always holds in the first quadrant of the ξ plane. Further, the imaginary parts of $g_1(v_{\pm 1})$ and $g_1(v_0)$ may not all be equal, for then there could be no possibility of the contributions canceling to produce a zero. This requirement is not simple: on an analytic path of steepest descent the imaginary part of the function is constant. To produce a zero of χ by this mechanism, the path of steepest descent must go from $-\infty$ to the point $-\tau+i\sigma$ on the cut from $-\tau+i\sigma$ to $-\tau+i\infty$, via the saddle point v_{-1}, then round the cut to another point on it, then via an analytic contour over the saddle at $v=0$ to the other cut, round the cut to $\tau-i\sigma$, and then to $+\infty$ via the saddle point v_1. The parts of the contour from one point on a cut to another point on the cut are where the imaginary part of the function changes.

For a zero of χ of this second type in the first quadrant of ξ, Eq. (3.8a) shows that we must have either $\tau=\sigma-1/2$, $\sigma\geqslant 1/2$ or $\tau=1/2-\sigma$, $0\leqslant\sigma\leqslant 1/2$.

For $\tau = \sigma - 1/2$, $\sigma \geqslant 1/2$, a careful calculation of the values of $\mathrm{Im}[g_1(v)]$ on both sides of the cut from $-(\sigma - 1/2) + i\sigma$ to $-(\sigma - 1/2) + i\infty$ shows that a contour on which $\mathrm{Im}[g_1(v)] = \mathrm{Im}[g_1(0)]$ which passes through $v = 0$ cannot intersect the cut. Thus, for $\tau = \sigma - 1/2$ there is a continuous steepest descent contour from $-\infty$ to $+\infty$ which avoids both $v_{\pm 1}$ and the two cuts. Hence there are no zeros of this type for $\xi = \sigma + i(\sigma - 1/2)$ with $\sigma \geqslant 1/2$. On the other hand, for $\xi = \sigma + i(1/2 - \sigma)$, $0 \leqslant \sigma \leqslant 1/2$, the contour with $\mathrm{Im}[g_1(v)] = \mathrm{Im}[g_1(0)]$ through $v = 0$ does intersect the cuts.

In this case the contour of steepest descent goes from $v \to -\infty$ to $v = i\xi$ over the saddle point at v_{-1} {with $\mathrm{Im}[g_1(v)] = \sigma(1 - 2\sigma)$}, then up the right-hand side of the left-hand cut to a point $\bar{v}$ {$\mathrm{Im}[g_1(v)]$ changes from $\sigma(1 - 2\sigma)$ to $\sigma - 1/2$}, then from $\bar{v}$ to $-\bar{v}$ on the left-hand side of the right-hand cut {with $\mathrm{Im}[g_1(v)] = \sigma - 1/2$} over the saddle point at $v = 0$, then up the left-hand side of the right-hand cut from $-\bar{v}$ to $-i\xi$ {$\mathrm{Im}[g_1(v)]$ changes from $\sigma - 1/2$ to $\sigma(1 - 2\sigma)$}, and then from $-i\xi$ to $v \to +\infty$ over the saddle point at v_{+1} {with $\mathrm{Im}[g_1(v)] = \sigma(1 - 2\sigma)$}.

Thus, for

$$\xi = \sigma + i(\sigma - \tfrac{1}{2}), \qquad 0 \leqslant \sigma \leqslant \tfrac{1}{2} \tag{3.8c}$$

the three saddle points v_0, $v_{\pm 1}$ of $g_1(v)$ can produce a zero of $\chi(\xi, l)$.

If we now put $\xi = i\tau$ with $\tau > 1/2$, a standard steepest descent evaluation of the integrals of Eq. (3.2) gives

$$\chi(\xi, l) = 2\left(\frac{\pi}{l}\right)^{1/2} \cos(l\tau - \phi)\,[1 + O(l^{-1})] \tag{3.9}$$

where

$$\phi = \frac{1}{2}\arctan\left(\frac{1}{2\tau}\right) \tag{3.10}$$

Hence, for $n > l/2\pi$ there are partition function zeros at

$$\xi_n = i(n + \tfrac{1}{2} + \Delta_n)\pi/l[1 + O(l^{-1})] \tag{3.11}$$

where $0 \leqslant \Delta_n \leqslant 1/4$.

On the line $\xi = \sigma + \frac{1}{2}(\frac{1}{2} - \sigma)$, $0 \leqslant \sigma \leqslant \frac{1}{2}$, there are contributions from three saddle points to χ and a single evaluation gives

$$\chi(\xi, l) = 2e^{l\xi}\left(\frac{\pi\xi}{l(\xi - 1/2)}\right)^{1/2}\left[e^{l(\xi - 1/2)^2} + \frac{1}{2}\left(1 + \frac{1}{2\xi}\right)^{1/2}\right][1 + O(l^{-1})] \tag{3.12}$$

We then find zeros $\xi_m = 1/2 - \tau_m + i\tau_m$ with

$$\tau_m = \left[\left(m - \frac{1}{2}\pi/l\right)\right]^{1/2} [1 + O(l^{-1})] \qquad \text{for} \quad 0 \leqslant m \leqslant \frac{l}{4\pi} \tag{3.13}$$

The results in Eqs. (3.11) and (3.13) together with the symmetries $\xi \to -\xi$ and $\xi \to \xi^*$ give a complete description of the zeros of $\chi(\xi, l)$ in the ξ plane.

We may finally consider the density of zeros along the arcs in the complex ξ plane on which they lie. In the limit $l \to \infty$ we may write

$$\lim_{l \to \infty} (1/l) \log \chi(\xi, l) = \int_C \log[1 - \xi/\xi(s)]\, \rho(s)\, ds \tag{3.14}$$

where s is an arc length variable along the lines of zeros we have just found. On $\xi = i\tau$ for $\tau > 1/2$, $s = \tau$, $\xi(s) \leqslant is$, and the density is $\rho(s) = 1/\pi$, a constant. On $\xi = \sigma + i(1/2) - \sigma)$ for $0 \leqslant \sigma \leqslant 1/2$, $s = (1/2 - \sigma)\sqrt{2}$, $\xi(s) = 1/2 - (1 - i)s/\sqrt{2}$, and the density is $\rho(s) = s/\pi$ with $s = 0$ at $\xi = 1/2$. There are similar zero densities on the other arcs of zeros. We note that the zero density becomes zero at the critical value $\xi = 1/2$. We sketch the distribution of zeros in Fig. 1.

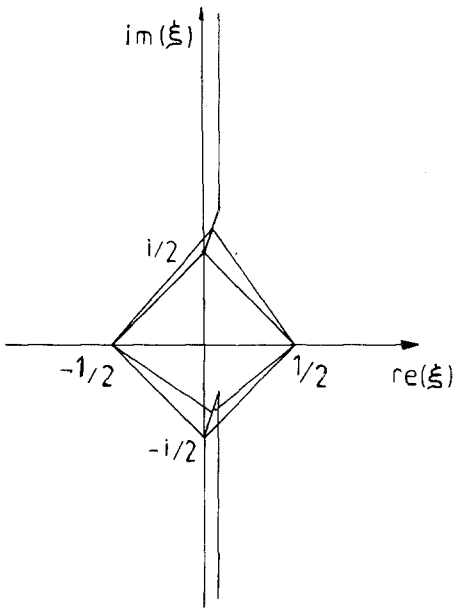

Fig. 1. Sketch of zeros and their densities for $\chi(\xi, l)$ as $l \to \infty$.

We may also note that the arcs of zeros cut the positive real ξ axis at $\xi = 1/2$ at an angle of $3\pi/4$, not $\pi/2$. The transition is in fact of mean field type and the angle $3\pi/4$ is in agreement with the theory developed by Glasser *et al.*[8] for the zeros of the finite-size scaling partition function. The variable $\xi = \zeta/\gamma$ is a coupling variable in this system, so that fugacity does not play the role envisaged in Yang–Lee theory and there is no expectation that the zero arcs should cut the axis at an angle of $\pi/2$.

4. FINITE-SIZE SCALING AND FIELD ZEROS

The critical point is at $\xi = 1/2$ and $\omega = 0$. Near this critical point the dominant contribution to the partition function Ξ of Eq. (2.15) comes from the term with $\exp[L(u^2 + \xi^2)^{1/2}]$. The saddle points of the exponent are all close to $u = 0$. We introduce the scaled variables

$$\kappa = (\gamma L)^{1/2}\left(\frac{1}{2\xi} - 1\right) \tag{4.1}$$

and

$$\Omega = (\gamma L)^{3/4}\omega \tag{4.2}$$

and define

$$F(\kappa, \Omega) = \lim_{L \to \infty} \frac{\Xi(\frac{1}{2}\gamma[1 - \kappa/(\gamma L)^{1/2}], L, \gamma, (\gamma L)^{-3/4}\Omega)\, \Gamma(1/4)}{2\Xi(\gamma/2, L, \gamma, 0)} \tag{4.3}$$

If we expand the exponent in the integrand in Eq. (2.15) to fourth order in u, introduce κ and Ω, and change the variable of integration to $v = u(\gamma L)^{1/4}$, we obtain

$$F(\kappa, \Omega) = \int_{-\infty}^{\infty} \exp(-u^4 + \kappa u^2 + \Omega u)\, du \tag{4.4}$$

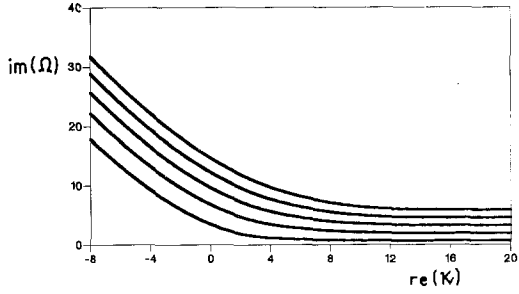

Fig. 2. Plot of $\mathrm{Im}[\Omega_n(\kappa)]$ for real κ for $n = 1$, 2, 3, 4, and 5.

which is the finite-size scaled partition for the system close to its critical points. It is a generic mean-field-theory partition function.[8]

In this section we consider κ real and find $\Omega_n(\kappa)$ defined by

$$F(\kappa, \Omega_n(\kappa)) = 0 \tag{4.5}$$

so that there are many branches n of $\Omega(\kappa)$.

Note that if $F(\kappa, \Omega) = 0$, then $F(\kappa, -\Omega) = 0$, $F(\kappa^*, \Omega^*) = 0$, and $F(\kappa^*, -\Omega^*) = 0$. We can construct an asymptotic expansion of $F(\kappa, \Omega)$ for large $|\Omega|$ in powers of $|\Omega|^{-1}$. The expansion produces zeros because the contour of steepest descent for real κ is divided in three parts (like Gaul), from $-\infty$ to $i\infty$, from $i\infty$ to $-i\infty$, and then from $-i\infty$ to ∞, each part crossing a saddle point. For $\kappa = 0$ the zeros are all pure imaginary, with, for $n \geqslant 1$,

$$\Omega_n(0) = 4i \left\{ \frac{2\pi}{3\sqrt{3}} \left(n - \frac{1}{3} \right) \right\}^{3/4} \left[1 + \frac{21}{64} \left[2\pi \left(n - \frac{1}{3} \right)^{-2} \right] \right.$$
$$\left. - \frac{147}{8912} \left[2\pi \left(n - \frac{1}{3} \right) \right]^{-4} + O(n^{-6}) \right] \tag{4.6}$$

There is no $\Omega_0(0)$, but the symmetries of F imply another set of zeros, $\Omega_n(0) = -\Omega_{-n}(0)$, for $n \leqslant -L$. For $n = 3$ this expansion and the numerical value differ by one in the fourth significant figure and for $n = 1$ this difference is two in the third significant figure. In Fig. 2 we plot the imaginary part of Ω_n as a function of real κ for both positive and negative κ. The real part of $\Omega_n(\kappa)$ is zero whenever κ is real. Note that increasing κ corresponds to increasing the coupling in the system. Thus, for real coupling the line of zeros in the finite-size scaled symmetry-breaking field Ω cuts the real axis at an angle of $\pi/2$, as might be expected from the Yang–Lee picture. Figure 2 also shows the partition function zeros pinching the real axis as the coupling increases through its critical value: the actual spacing in field between these zeros and the real axis is $O(L^{-3/4})$.

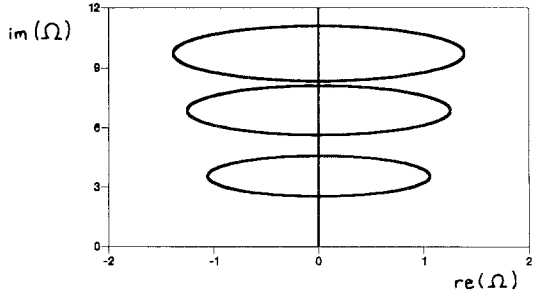

Fig. 3. Plot of trajectory $\Omega_n(ke^{i\phi})$ for $n = 1, 2, 3$ for $k = 1$.

5. ZEROS IN BOTH VARIABLES

In this section we present numerical data on the motion of the zeros $\Omega_n(\kappa)$ in the complex Ω plane for κ a complex variable. We take $\kappa = ke^{i\phi}$, $0 \leqslant \phi \leqslant 2\pi$, and plot the trajectories of the $\Omega_n(ke^{i\phi})$. To aid this discussion, we call the solutions of $F(\kappa, 0) = 0$, $\kappa_m = k_m e^{i\phi_m}$ with k_m and ϕ_m real. These κ_m have been discussed in some detail by Glasser *et al.*[9]

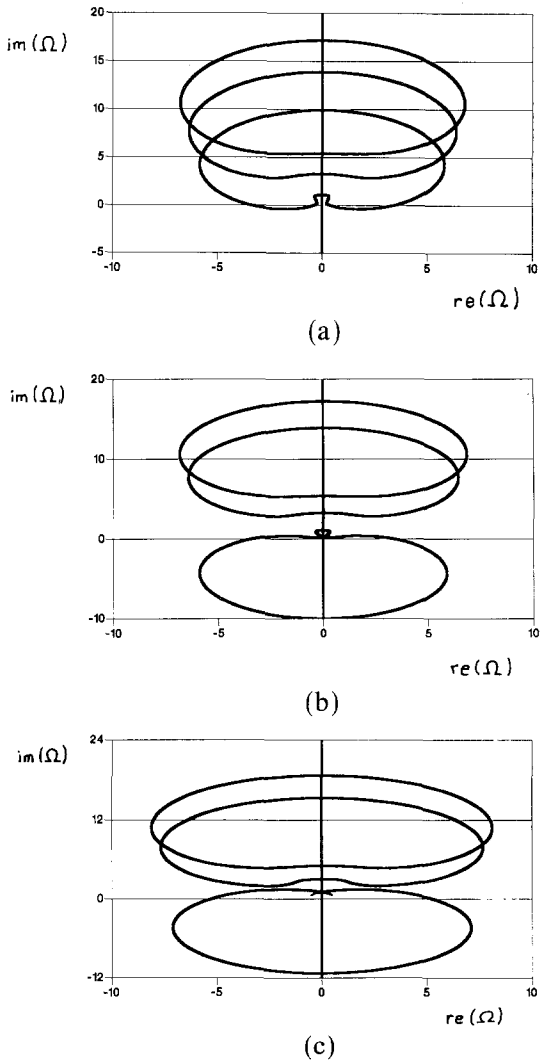

Fig. 4. Plot of trajectories of $\Omega_n(ke^{i\phi})$ for $n = 1, 2, 3$ for (a) $k = 4.35$, (b) $k = 4.385$, (c) $k = 5.05$.

First we consider k small compared with k_1. At $\phi = 0$ we have zeros $\Omega_n(0)$ which can be read off the graph in Fig. 2. As ϕ increases, we expect $\Omega_n(ke^{i\phi})$ to move in a loop with $\mathrm{Re}(\Omega_n) > 0$ to begin and then return to the imaginary axis at $\phi = \pi$ at a larger value of $\mathrm{Im}(\Omega_m)$, with a symmetric loop returning to $\Omega_n(\kappa)$. This is shown in Fig. 3 for the zeros Ω_1, Ω_2, and Ω_3. There are also zeros, not drawn, $\Omega_{-n}(ke^{i\phi}) = -\Omega_n(ke^{i\phi})$. The zeros in Figs. 3–6 are all for $n = 1, 2, 3$ from bottom to top.

As k increases to k_1, these loops must become more complicated, since at $\kappa = k_m e^{i\phi_m}$, $\Omega_m = 0$. Thus the loop trajectory of Ω_1 must dent at the bottom and the edges of the dent close into the origin. If we have $\kappa = \kappa_m e^{i(\phi_m + \delta\phi)}$, then we have, for small Ω,

$$F(\kappa_m, \Omega) \simeq \left(\frac{1}{2}\Omega_m^2 + i\kappa_m \delta\phi\right) \int_{-\infty}^{\infty} u^2 e^{u^4 + \kappa_m u^2} du \tag{5.1}$$

so that the trajectory crosses itself at $\delta\phi = 0$. In Figs. 4a and 4b we show the trajectories for $k < k_1$ and $k > k_1$ and $k_1 \simeq 4.38$. In Fig. 4b, the loop of $\Omega_1(\kappa)$ has inverted itself and has a small subloop on top. This subloop gets

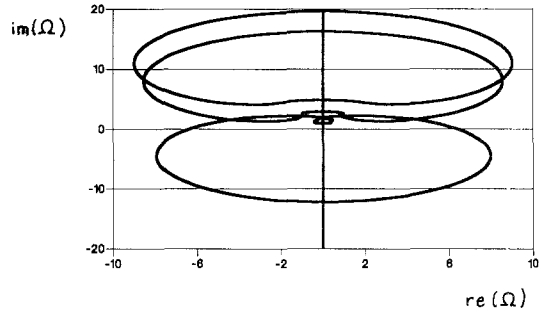

(a)

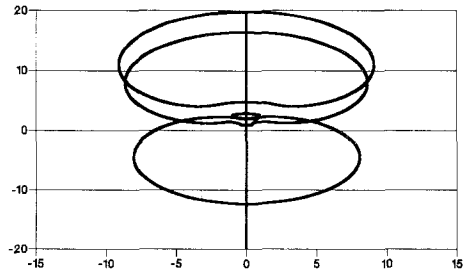

(b)

Fig. 5. Plot of trajectories of $\Omega_n(ke^{i\phi})$ for $n = 1, 2, 3$ for (a) $k = 5.5$, (b) $k = 5.55$.

drawn tighter as k increases to $k \simeq 4.95$, when the trajectory has a cusp because $\partial F/\partial \Omega = 0$ on the trajectory. This is shown in Fig. 4c for $k = 5.05$, where the turning point is not singular, but very sharp and more obvious.

It should be noted that these graphs of trajectories should be augmented by the graphs of Ω_{-1}, Ω_{-2}, Ω_{-3}.

As k increases further toward k_2, the loop of Ω_2 also becomes dented on the bottom. A crossover phenomenon occurs near $k = 5.5$ (when $\partial F/\partial \kappa = 0$) between this developing dent and the subloop from the Ω_1 trajectory. This

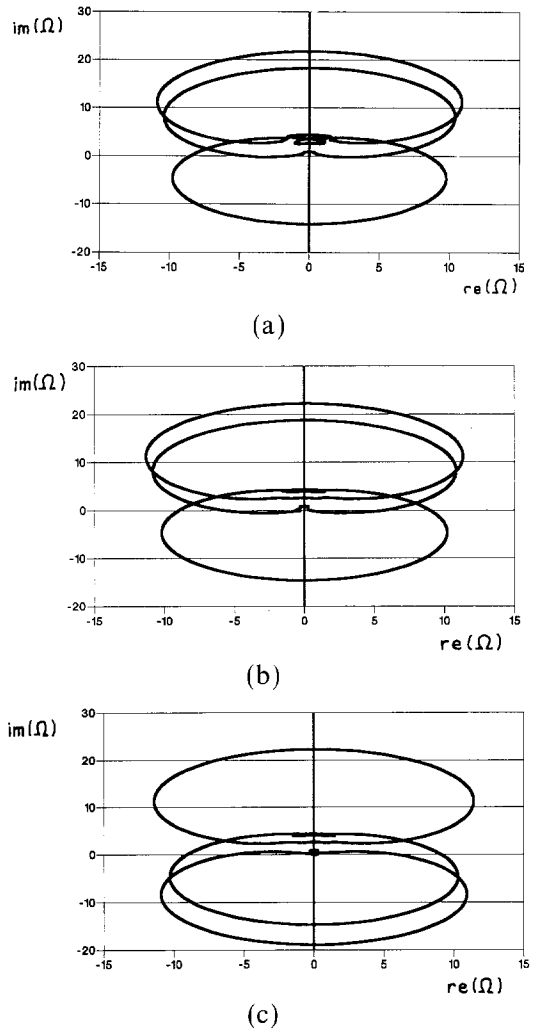

Fig. 6. Plot of trajectories of $\Omega_n(ke^{i\phi})$ for $n = 1, 2, 3$ for (a) $k = 6.4$, (b) $k = 6.6$, (c) $k = 6.65$.

is shown in Figs. 5a and 5b. This crossover flattens out the dent in the bottom of the Ω_2 trajectory and leaves a "knot" in the Ω_1 trajectory. The dent in the Ω_2 trajectory then develops further, pinching into the origin at $k = k_2 \simeq 6.6$. Meanwhile, a crossover phenomenon occurs between the Ω_1 and Ω_3 loops. These are shown in Figs. 6a–6c. Each Ω_m trajectory inverts (with an upper subloop) as k passes k_m. The general structure of the Ω_n trajectories is then fairly clear.

Perhaps the most interesting feature of these trajectories is their quite extraordinary richness in behavior, which suggests that similar studies in the joint complex coupling–complex field space for more complex phase transitions would be very interesting.

ACKNOWLEDGMENTS

The authors acknowledge financial support from the Danish Technical Science Research Council's FTU program (grant number 5.17.2.6.21), the Danish Natural Science Research Council (grant number 11-83541), and the Esprit program of the European Community (grant number PCA 4026).

REFERENCES

1. C. N. Yang and T. D. Lee, *Phys. Rev.* **87**:407 (1952).
2. T. D. Lee and C. N. Yang, *Phys. Rev.* **87**:410 (1952).
3. O. Penrose, *J. Math. Phys.* **4**:1312 (1963).
4. M. E. Fisher, in *Lectures in Theoretical Physics VIIC* (University of Colorado Press, Boulder, Colorado, 1965).
5. P. J. Forrester, *J. Stat. Phys.* **51**:457 (1988).
6. P. J. Forrester, *J. Stat. Phys.* **54**:57 (1989).
7. C. Itzykson, R. B. Pearson, and J. B. Zuber, *Nucl. Phys. B* **220**:415 (1983).
8. M. L. Glasser, V. Privman, and L. S. Schulman, *Phys. Rev. B* **35**:1841 (1987).
9. M. L. Glasser, V. Privman, and L. S. Shulman, *J. Stat. Phys.* **45**:451 (1986).
10. E. R. Smith and P. J. Forrester, *Helv. Phys. Acta* **62**:1004 (1989).